ARTICLE

Ion Pairing Kinetics Does not Necessarily Follow the Eigen-Tamm Mechanism[†]

Qiang Zhang[a,b], Bing-bing Zhang[b,c], Ling Jiang[b*], Wei Zhuang[b*]

a. Department of Chemistry, Bohai University, Jinzhou 121000, China
b. State Key Laboratory of Molecular Reaction Dynamics, Dalian Institute of Chemical Physics, Chinese Academy of Sciences, Dalian 116023, China
c. College of Chemistry and Molecular Engineering, Zhengzhou University, Zhengzhou 450001, China

The most recognized and employed model of the solvation equilibration in the ionic solutions was proposed by Eigen and Tamm, in which there are four major states for an ion pair in the solution: the completely solvated state, 2SIP (double solvent separate ion pair), SIP (single solvent separate ion pair), and CIP (contact ion pair). Eigen and Tamm suggested that the transition from SIP to CIP is always the slowest step during the whole pairing process, due to a high free energy barrier between these two states. We carried out a series of potential of mean force calculations to study the pairing free energy profiles of two sets of model mono-atomic 1:1 ion pairs $2.0{:}x$ and $x{:}2.0$. For $2.0{:}x$ pairs the free energy barrier between the SIP and CIP states is largely reduced due to the salvation shell water structure. For these pairs the SIP to CIP transition is thus not the slowest step in the ion pair formation course. This is a deviation from the Eigen-Tamm model.

Key words: Ion pairing, Eigen-Tamm model, Potential of mean force

I. INTRODUCTION

Ion pairing is a topic of great importance in the physical, chemical, and biological sciences [1−10]. The specific binding of different metal cations to the negatively charged areas in the proteins can stabilize or destabilize the protein structures [8, 10−12], which is associated with a wide range of serious diseases, for instance, the misfolding of a chloride-selective channel, which is related to cystic fibrosis [11]. The formation of precipitation in water solution is usually described by the nucleation and growth theory, but more complex pathways have recently been proposed, such as aggregational processes of nanoparticle precursors or pre-nucleation clusters, which seem to contradict the classical theory [12]. Studying the ion pairing preferences in various environments can help to improve our understanding of the physics underlying these phenomena.

Molecular dynamics (MD) simulation can provide a detailed picture for the properties in the ionic solutions at molecule level. The perturbation of ion on the structures and dynamics of water, as well as the specific effect of ion on the functions of biosystems have been explored extensively [13−26] by the MD simulations. The recent studies show that the effect of ion pairing plays an important role in the solvent structure [13, 2−8]. The equilibrium constants of ion pairing in aqueous alkali halide solutions have been studied systematically by MD simulations and discussed in comparison with the experimental measurements [1, 27]. The dynamic properties of NaCl clusers are also explored in previous works [4, 5]. Dill and co-workers carried out the MD simulations to calculate the potentials of mean force (PMF) for the alkali halide ion pairs in the infinitely diluted aqueous solutions [7].

The most recognized and employed model of the solvation equilibration in the ionic solutions was proposed by Eigen and Tamm [1, 28], in which there are four major states for an ion pair in the solution: the completely solvated state, 2SIP (double solvent separate ion pair), SIP (single solvent separate ion pair), and CIP (contact ion pair). Eigen and Tamm suggested that the transition from SIP to CIP is always the slowest step during the whole pairing process, which is due to a high free energy barrier between these two states.

In this work, we carried out a series of MD based PMF calculations to study the pairing preferences of the model mono-atomic 1:1 ions with evenly varied sizes (2.0 Å to 6.0 Å for cation, 2.0 Å to 6.0 Å for anion, with a 1 Å increment), we found that the solvation equilibration of the "big anion-small cation" pairs is consistent with Eigen-Tamm model, but there is a deviation for the "small anion-big cation" pairs. This is again mainly due to the different water bridging structures of differ-

ent ion pairs.

To demonstrate that the asymmetry in the water structure plays an important role in the kinetics of the ion pairing phenomenon, we used the widely accepted non-polarizable force field models in the PMF calculations. The role of polarizability in this phenomenon is an interesting topic, but is out of the scope of this work. We don't expect other force fields will give major difference in the conclusion.

II. METHODS

A. Molecular dynamics simulation

The SPC/E model [29] is used for the water molecules in the current simulations. The model ions with unit positive or negative charge and various sizes are used to explore the ion pairing tendency in water solution. The Lennard-Jones 12-6 form is selected as the vdW interactions of ion-ion and ion-water:

$$u_{ij} = 4\varepsilon_{ij}\left[\left(\frac{\sigma_{ij}}{r_{ij}}\right)^{12} - \left(\frac{\sigma_{ij}}{r_{ij}}\right)^{6}\right] + \frac{q_i q_j}{4\pi\varepsilon_0 r_{ij}} \quad (1)$$

The ion potential parameter ε is defined to be 0.42 kJ/mol, which is well used for most mono-valence ions in the Dang series [2, 30, 31] combined with SPC/E water (Table I). In the current work σ_{ij} varies from 2.0 Å to 6.0 Å for the cations and from 2.0 Å to 6.0 Å for the anions, with a step of 1 Å. The Lorentz-Berthelot rules [31, 32] were used for the combined Lennard-Jones potential parameters. The masses of the model cation and anion are fixed at values of Na and Cl. The effect of ion mass on the ion pairing is not considered here. For convenience, an ion pair with radius size R_A for anion and R_B for cation is denoted as R_A:R_B in the following text.

The thermodynamic properties of ion pairing can be studied using the PMF calculations. A series of constrained molecular dynamic simulations, with a fixed separation between the cation and the anion, were carried out at 298 K and 1 atm to estimate the PMF of an ion pair in the infinitely diluted aqueous solution. The separation between the cation and the anion was varied from 1.0 Å to 10 Å with a 0.2 Å increment. The SHAKE algorithm [33] was used to fix the separation of cation-anion in a specific simulation. A 6 ns simulation was carried out at each separation r to obtain the mean force after a 1 ns equilibration. The force imposed on the ion pair was recorded at every step (2 fs). The Nose-Hoover thermostat [34] was used with the coupling time constant of 1 ps. The periodic boundary condition and minimum image convention were adopted. The non-bonded van der Waals interactions were truncated at 10 Å with switching function and the particle mesh Ewald summation technique [35] was used to treat the long-range Coulomb interaction. The simulation trajectories were saved every 100 fs to extract the structural

TABLE I Force field parameters of halide and alkali ions and model ions including $R_{\text{I-Ow}}$ (distance between the ion and water oxygen from Ref.[31]) and $R_{\min}$ (the first minimum of radial distribution function of ion water pair).

Ion	σ/Å	$R_{\text{I-Ow}}$/Å	$R_{\min}$/Å
Cation	2.0	1.95	3.00
	3.0	2.65	3.55
	4.0	3.15	4.10
	5.0	3.75	5.45
	6.0	4.35	6.20
Anion	2.0	2.05	2.70
	3.0	2.55	3.15
	4.0	3.05	3.65
	5.0	3.55	4.15
	6.0	4.05	4.65

information. All simulations were performed with the Tinker simulation code [36].

The mean force imposed on the ions is the sum of the forces exerted by the water molecules $\Delta F(r)$ and the direct force $F_d(r)$ between ions [2, 7, 37−39].

$$F(r) = F_d(r) + \Delta F(r) \quad (2)$$

$\Delta F(r)$ can be expressed as

$$\Delta F(r) = \frac{1}{2}\langle \mathbf{r}_p \cdot (\mathbf{F}_{\text{AS}} - \mathbf{F}_{\text{BS}})\rangle \quad (3)$$

where $\mathbf{F}_{\text{AS}}$ and $\mathbf{F}_{\text{BS}}$ are the forces imposed on the ions by the water molecules and $\mathbf{r}_p$ is a unit vector of the connecting line of ion pair. The PMF at distance r relative to r_0, $W(r)$ was obtained by the integration of the total force.

$$W(r) = W(r_0) - \int_{r_0}^{r} F(r)\mathrm{d}r \quad (4)$$

In which $W(r_0)$ is PMF value of ion pair at the separation of r_0. The upper limit r_0 of the integration was taken to be 10 Å, at which the PMF almost changes inversely with the distance of ion pair [7]. The screening Coulomb potential $W(r)$ was used as the PMF value when the separation of ion pair is beyond r_0 as in the previous work [2].

$$W(r) = \frac{q_i q_j}{\varepsilon_r r} \quad (5)$$

The q_i and q_j are the ionic charges and ε_r is the dielectric constant of pure water at standard condition (ε_r=78) [40]. Fixing the ion-ion distance introduces an artificial force $-2k_B T/r$ [41, 42], which needs to be taken into account in the PMF calculations, thus the total PMF can be expressed as:

$$W(r) = -\int_{r_0}^{r} \mathbf{F}(r')\mathrm{d}r' + 2k_B T \ln\left(\frac{r}{r_0}\right) + W(r_0) \quad (6)$$

B. Ion pairing entropy and enthalpy

We can further decompose PMF into entropy and enthalpy contributions as:

$$W(r) = \Delta H(r) - T\Delta S(r) \tag{7}$$

The relative entropy and enthalpy differences of the system at distance r to r_0 (10 Å), can be derived from the following relationship [43]:

$$
\begin{aligned}
\Delta S(r) &= -\frac{\partial W(r)}{\partial T} \\
&\approx \frac{-W_{T+\Delta T}(r) - W_T(r)}{\Delta T}
\end{aligned}
\tag{8}
$$

$$
\begin{aligned}
\Delta H(r) &= -\frac{\partial W(r)/T}{\partial(1/T)} \\
&\approx W(r) + T\Delta S(r)
\end{aligned}
\tag{9}
$$

We calculated $W(r)$ at 285, 298, and 310 K, based on which the numerical derivatives of $W(r)$ with respect to T were evaluated.

C. The coordination numbers and density of water around ion pair

The water bridging structures play an important role in the stability of ion pair. In order to visualize the solvation structures of ion pair at the different solvation states, the two-dimension densities of water oxygen around the ion pair were analyzed. The spherical radius of ion solvation shell is defined as the first minimum of the pair radial distribution function (RDF) of ion-water oxygen (Table I). The bridging water of ion pair is defined as the water, whose oxygen locates both in solvation shells of cation and anion at same time. The bridging water number of ion pair is labeled as N_P. Additionally, the transition state (TS) from SIP to CIP is defined as the separation of ion pair at the maximum of PMF between the SIP and CIP. The structure of TS can provide connective information of pairing path.

D. The potential energies of subsystems in solutions

In order to calculate the decomposed energies of subsystems, we used the generalized reaction field (GRF) method [44] to treat the Coulombic long-range interactions instead of the Ewald summation technique. The trajectories from the NPT simulation with the Ewald summation technique as main text were used to calculate the potential energies of subsystems in the solutions. With this routine, the total potential of solution (E_T), the pair potential of anion and cation (E_I), and the remaining part of E_R (water reorganization energy), as well as the potential of water within the solvation shells of ion pair (E_S) and the potential of water beyond the solvation shells of ion pair (E_B), were calculated.
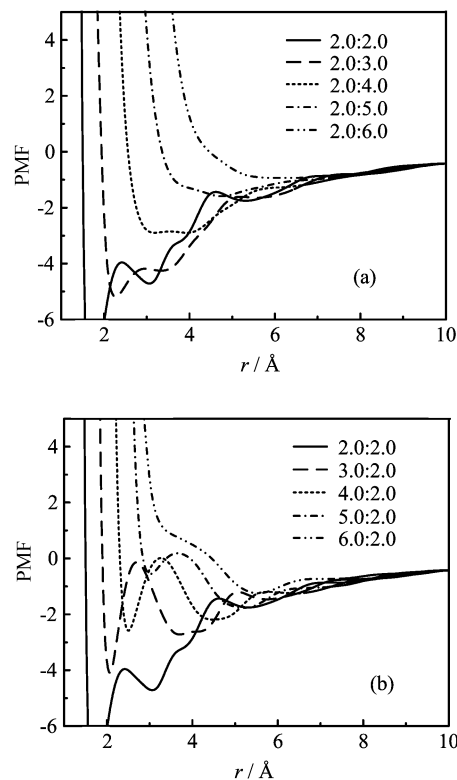
FIG. 1 PMFs for (a) 2.0:x and (b) x:2.0 ion pairs.

III. RESULTS

The PMFs of 2.0:x and x:2.0 ion pair series are presented in Fig.1. The first minimum of PMF (the position of CIP) decreases with the increment of the size of ion x. An evident difference between the 2.0:x and x:2.0 ion pairs is that higher transition barriers from SIP to CIP are observed for x:2.0 pairs than 2.0:x pairs. In Fig.2, we further decomposed the PMFs into the entropy and the enthalpy contributions for two representative ion pairs, 2.0:3.0 and 3.0:2.0. When the ions approach each other, the entropy has the similar increasing behavior, while the enthalpy behaves differently for the two pairs. The enthalpy of 2.0:3.0 ion pair decreases more evidently at SIP than 3.0:2.0 ion pair.

The enthalpy change is closely related to the reorganization of the water bridging structures from SIP to CIP. For the 2.0:3.0 and 3.0:2.0 ion pairs, two-dimension density distribution of the bridging water and the suggested water-bridging structures at SIP, TS, and CIP are presented in Fig.3. Interestingly, the distribution splits into two separate regions at CIP for the 3.0:2.0 ion pair.

We further plotted the distributions of α and β angles (defined as in Fig.4) for the 2.0:3.0 and 3.0:2.0 ion pairs in Fig.5. The distribution of α is broader than that of β since the anion has stronger restriction on the OH orientation of water than the cation with similar size
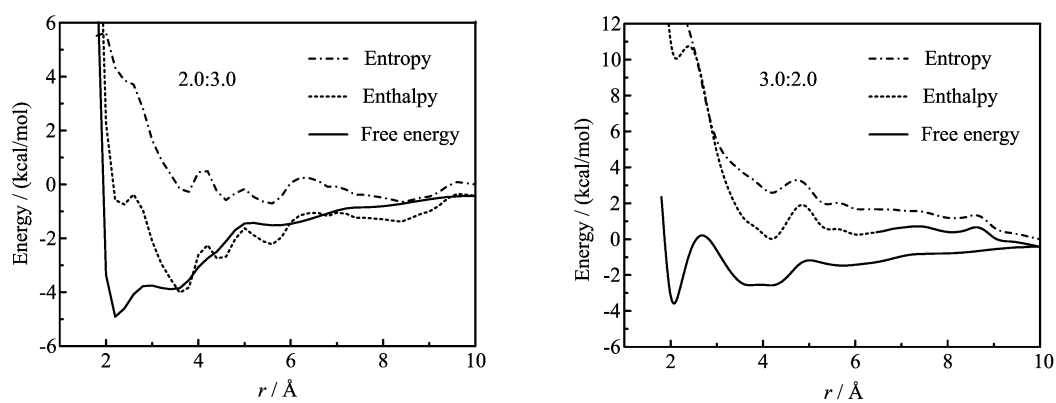
FIG. 2 The relative free energies, relative enthalpies, and relative entropies of 2.0:3.0 and 3.0:2.0 ion pairs.
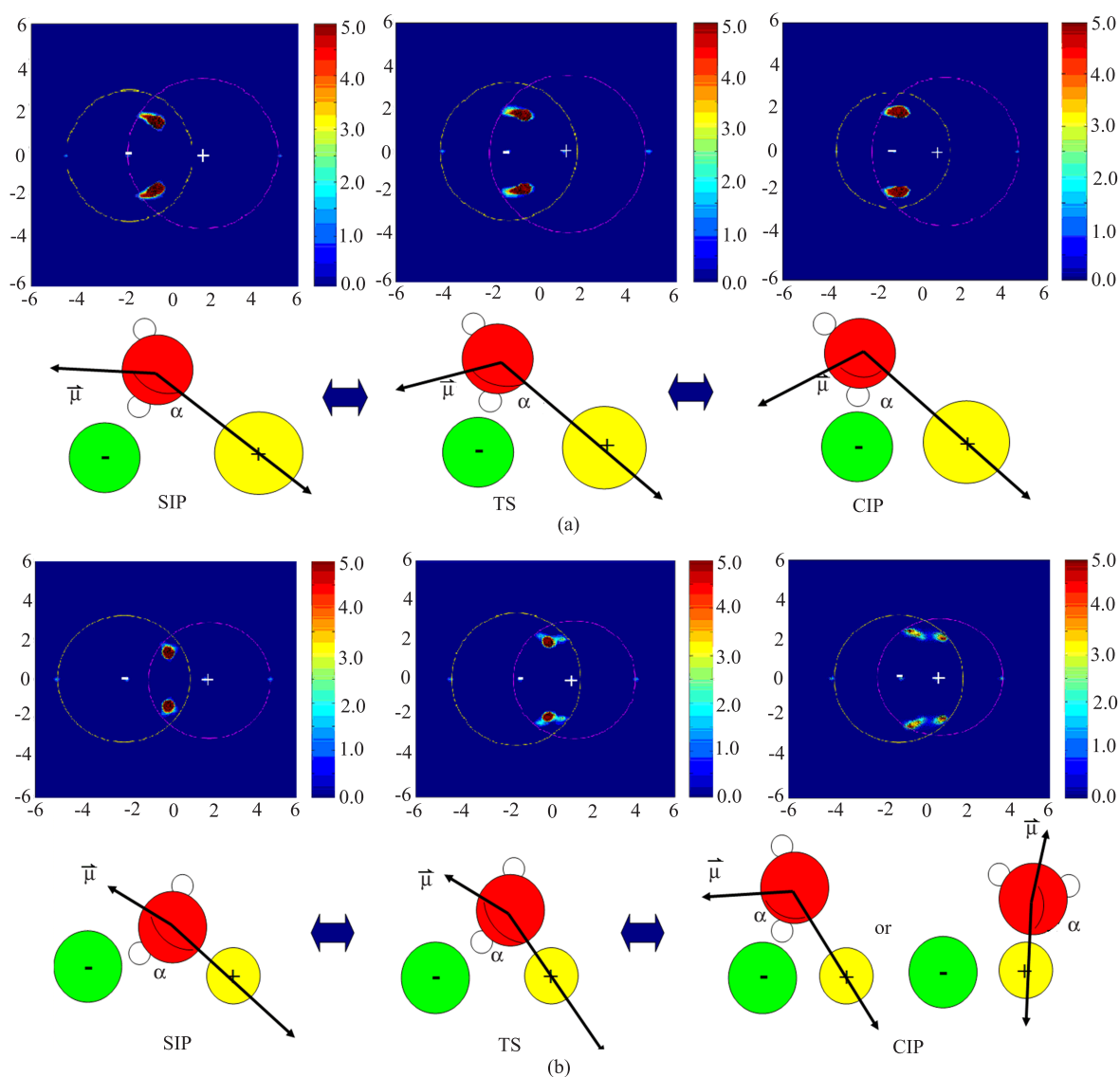
FIG. 3 The water oxygen densities and the schematic configures of the water-bridging ion pair around (a) 2.0:3.0 and (b) 3.0:2.0 ion pairs at the CIP, TS (transition state), and SIP. The circle shows the radius of ions with the values in Table I.
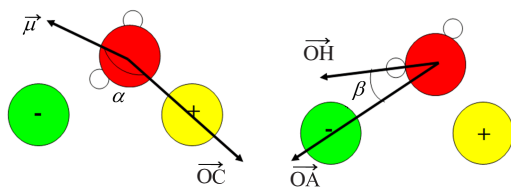
FIG. 4 The dipole orientation of water is defined as the angle α, which is the product of dipole vector $\vec{\mu}$ and cation-water oxygen vector $\overrightarrow{OC}$. The OH orientation is defined as the angle β, which are the product of $\overrightarrow{OH}$ and anion-water oxygen vector $\overrightarrow{OA}$.

TABLE II The decomposed potential energies at the different states of 2.0:3.0 and 3.0:2.0 ion pairs relative to the values of ion pair at 10 Å (0 kcal/mol). The subsystem energies are defined in method part (unit: kcal/mol) in Section II.

Ion pair		E_T	E_I	E_B	E_R	E_S
3.0:2.0	CIP	2.15	−86.56	−38.72	88.81	127.43
	TS	5.78	−55.33	−29.71	61.11	90.82
	SIP	1.81	−21.54	−15.65	23.35	39.00
2.0:3.0	CIP	−0.29	−75.62	−38.98	75.33	114.31
	TS	0.42	−47.25	−30.62	48.67	78.29
	SIP	−0.69	−29.52	−18.64	28.83	47.47

on the dipole orientation of water. For 2.0:3.0, from 10 Å to CIP, part of α distribution continuously shifts to the lower value. Among which the major contribution comes from the bridging water, especially at the CIP state. For 3.0:2.0, on the other hand, when the pair moves from TS to CIP, the α distribution of the bridging water is apparently split, part shifts further to the lower value, and part returns to the higher value. This suggests a heterogeneous configuration distribution of the water bridging structure, which explains the observation in the two dimensional density distribution of water oxygen in Fig.3. The small cation with size 2.0 Å has stronger restrain on the dipole orientation of the bridging waters, so it becomes harder to maintain the bridging water configuration at CIP. Some of the water molecules between the ions (counted as "bridging water") thus have their bridging structure broken, move closer to the cation and eventually become the cation-bound water solely. The facts above suggest that an evident reorganization of solvation structure takes place from TS to CIP for 3.0:2.0 ion pair.

To understand the enthalpy difference between the 3.0:2.0 and 2.0:3.0 pairs, we decomposed the total potential energy E_T into cation-anion pair potential energy and the reorganization energy of water as (in Table II):

$$E_T = E_R + E_I$$
$$= E_S + E_B + E_I \quad (10)$$

For both pairs, E_I decreases monotonically for both pairs from 10 Å to CIP due to the reduction of ion pair separation, but a continuous increment for E_R and E_S, more evident for 3.0:2.0 ion pair than 2.0:3.0 ion pair. The changes of $E_R + E_I$ are −29.71 and −47.85 kcal/mol for 2.0:3.0 and 3.0:2.0 ion pairs, correspondingly 30.82 and 51.82 kcal/mol for those of E_S. The tendency of change for $E_B + E_I$ is opposite to that of E_S. This shows that bigger increment of total energy should come from the solvation shell waters of ion pair. More intense and uncomfortable structures of the bridging water are suggested for the 3.0:2.0 ion pair at TS state than 2.0:3.0 ion pair. The orientation of water dipole around 3.0:2.0 ion pair shifts back to the preferred orientation of bridging water from TS to CIP. This also suggests that a

more remarkable reorganization of solvation structure takes place from TS to CIP for 3.0:2.0 ion pair than 2.0:3.0 ion pair, which can be observed from Fig.5.

IV. DISCUSSION

The reputable Eigen-Tamm model suggests that transition from SIP to CIP is always the slowest step in the whole pairing process [1, 28]. In our simulation, we observed different pairing free energy profiles for the small anion-large cation pairs and the large anion-small cation pairs. Using the 2.0:x and x:2.0 series as an example (Fig.1), the PMF curves for the x:2.0 series have significant barriers between SIP and CIP, thus their SIP to CIP transitions should be the slowest step, which is consistent with the Eigen-Tamm model. The PMF curves of the 2.0:x series, on the other hand, do not have significant free energy barriers between the SIP and CIP states. For these pairs there is only negligible free energy barrier between SIP to CIP. And the SIP to CIP transition is not necessarily the slowest step during the whole pairing process.

The low free energy barrier between SIP and CIP observed in 2.0:x is the consequence of the ion pair solvation structures. To demonstrate this, we examined the hydration structures of the 2.0:3.0 and 3.0:2.0 pairs. The entropy profiles of these two pairs are similar to each other, so the differences in their PMF profiles are dominated by the largely different enthalpy profiles. For 2.0:3.0 the maximum of the α distribution for the bridging water at TS only shifts to the value of ~10° lower compared with that at SIP. This induces a mild increase of enthalpy almost completely cancelled by the entropy increase. A rather flat SIP-to-TS segment is thus observed in the PMF profile. For 3.0:2.0, on the other hand, the shift is more than 30° to lower value, which causes a much more drastic enthalpy increase only partly cancelled by the entropy increase. A monotonically rising SIP-to-TS segment is thus observed in the PMF profile. From TS to CIP, both pairs have a dominant increasing entropy effect, which creates a decreasing TS-to-CIP PMF segment. The different water
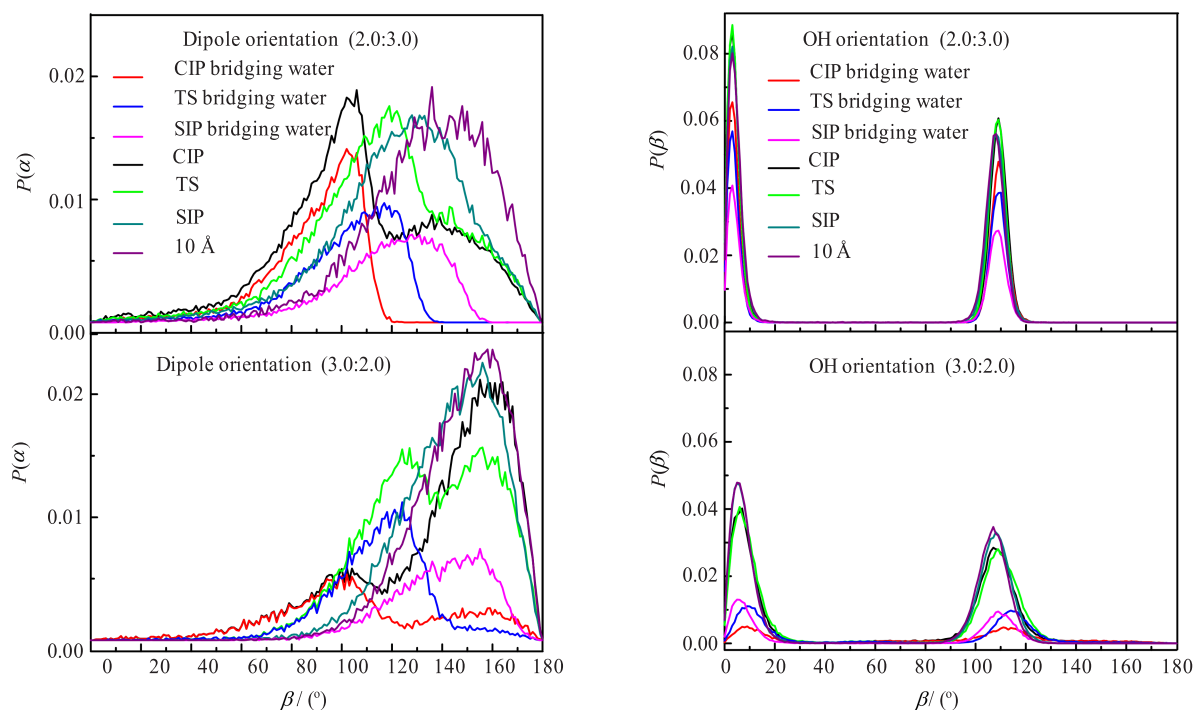
FIG. 5 The dipole and OH bond orientations of water in the cation and anion solvation shells for 2.0:3.0 and 3.0:2.0 ion pairs at CIP, TS, and SIP states. The orientations of bridging water are also shown separately.

bridging structures thus affect the pairing kinetics of these two pairs by generating a significant barrier for 3.0:2.0 and a rather downhill curve for 2.0:3.0 in the SIP-to-CIP segments of their PMF profiles.

Comparing the changes of subsystem energies for two ion pairs, we can clearly find the solvation shell waters play a key role in the transition barrier at TS. The changes of (E_B+E_I) are -29.71 and -47.85 kcal/mol for 2.0:3.0 and 3.0:2.0 ion pairs, correspondingly 30.82 and 51.82 kcal/mol for those of E_S. Besides this, the tendency of the former is opposite to the later. The higher barrier at TS is due to the structural differences of solvation shell waters of two ion pairs. More intense and uncomfortable structures of the bridging water are suggested for the 3.0:2.0 ion pair at TS state than 2.0:3.0 ion pair. The orientation of water dipole around 3.0:2.0 ion pair shifts back to the preferred orientation of bridging water from TS to CIP. This also suggests that there is a more remarkable reorganization of solvation structure from TS to CIP for 3.0:2.0 ion pair than 2.0:3.0 ion pair.

V. CONCLUSION

The water bridging structure eliminates the free energy barrier between SIP and CIP for certain ions pairs. For these pairs, the SIP to CIP transition is no longer the slowest step in the pairing process, which is a deviation from the well known Eigen-Tamm model. Our study thus suggested that the water bridging struc-

ture has an important influence on the ion pairing phenomenon, both thermodynamically and kinetically.

[1] Y. Marcus, Chem. Rev. **109**, 1346 (2009).
[2] D. E. Smith and L. X. Dang, J. Chem. Phys. **100**, 3757 (1994).
[3] L. Degrève and F. L. B. da Silva, J. Chem. Phys. **111**, 5150 (1999).
[4] A. A. Chen and R. V. Pappu, J. Phys. Chem. B **111**, 6469 (2007).
[5] S. A. Hassan, J. Phys. Chem. B **112**, 10573 (2008).
[6] B. Gu, F. S. Zhang, Z. P. Wang, and H. Y. Zhou, J. Chem. Phys. **129**, 184505 (2008).
[7] C. J. Fennell, A. Bizjak, V. Vlachy, and K. A. Dill, J. Phys. Chem. B **113**, 6782 (2009).
[8] (a) L. J. Yang, Y. B. Fan, and Y. Q. Gao, J. Phys. Chem. B **115**, 12456 (2011).

(b) Q. Zhang, W. Xie, H. Bian, Y. Q. Gao, J. Zheng, and W. Zhuang, J. Phys. Chem. B **117**, 2992 (2013).

[9] P. Jungwirth and D. J. Tobias, Chem. Rev. **106**, 1259 (2006).

[10] K. B. Rembert, J. Paterová, J. Heyda, C. Hilty, P. Jungwirth, and P. S. Cremer, J. Am. Chem. Soc. **134**, 10039 (2012).

[11] B. H. Qu, E. Strickland, and P. J. Thomas, J. Bioenerg. Biomembr. **29**, 483 (1997).

[12] A. Nordlund, L. Leinartaite, K. Saraboji, C. Aisenbrey, G. Gröbner, P. Zetterström, and J. Danielsson, Proc. Natl. Acad. Sci. USA **106**, 9667 (2009).

[13] (a) K. D. Collins and M. W. Q. Washabaugh, Rev. Biophys. **18**, 323 (1985).
(b) K. D. Collins, Biophys. J. **72**, 65 (1997).
(c) K. D. Collins, G. W. Neilson, and J. E. Enderby, Biophys. Chem. **128**, 95 (2007).
(d) K. D. Collins, Methods **34**, 300 (2004).

[14] A. Chandra, Phys. Rev. Lett. **85**, 768 (2000).

[15] A. P. Lyubartsev, K. Laasonen, and A. Laasonen, J. Chem. Phys. **114**, 3120 (2001).

[16] M. Carrillo-Tripp, H. Saint-Martin, and I. Ortega-Blake, J. Chem. Phys. **118**, 7062 (2003).

[17] N. Galamba, J. Phys. Chem. B **116**, 5242 (2012).

[18] P. Jungwirth and D. J. Tobias, Chem. Rev. **106**, 1259 (2006).

[19] P. Lo Nostro and B. W. Ninham, Chem. Rev. **112**, 2286 (2012).

[20] A. Kalra, N. Tugcu, S. M. Cramer, and S. Garde, J. Phys. Chem. B **105**, 6380 (2001).

[21] R. Zangi, J. Phys. Chem. B **114**, 643 (2010).

[22] B. Hessa and N. F. A. van der Vegt, PNAS **106**, 13296 (2009).

[23] R. L. Baldwin, Biophys. J. **71**, 2056 (1996).

[24] D. H. Min, H. Z. Li, G. H. Li, B. A. Berg, M. O. Fenley, and W. Yang, Chem. Phys. Lett. **454**, 391 (2008).

[25] Y. Zhang and P. Cremer, Model Systems/Biopolymers **10**, 658 (2006).

[26] K. Rembert, J. Paterova, J. Heyda, C. Hilty, P. Jung-wirth, and P. S. Cremer, J. Am. Chem. Soc. **134**, 10039 (2012).

[27] R. M. Fuoss, Proc. Natl. Acad. Sci. USA **77**, 34 (1980).

[28] (a) M. Eigen and K. Z. Tamm, Elektrochem. **66**, 93 (1962).
(b) M. Eigen and K. Z. Tamm, Elektrochem. **66**, 107 (1962).

[29] H. J. C. Berendsen, J. R. Grigera, and T. P. Straatsma, J. Phys. Chem. **91**, 6269 (1987).

[30] S. H. Lee and J. C. Rasaiah, J. Phys. Chem. **100**, 1420 (1996).

[31] D. Horinek, S. I. Mamatkulov, and R. R. Netz, J. Chem. Phys. **130**, 124507 (2009).

[32] M. P. Allen and D. J. Tildesley, *Computer Simulation of Liquids*, Oxford: Clarendon Press, (1987).

[33] H. C. Andersen, J. Comput. Phys. **52**, 24 (1983).

[34] (a) S. Nosé, Mol. Phys. **52**, 255 (1984).
(b) W. G. Hoover, Phys. Rev. A **31**, 1695 (1985).

[35] U. Essmann, L. Perera, M. L. Berkowitz, T. Darden, H. Lee, and L. G. Pedersen, J. Chem. Phys. **103**, 8577 (1995).

[36] J. W. Ponder and F. M. Richards, J. Comput. Chem. **8**, 1016 (1987).

[37] J. Timko, D. Bucher, and S. Kuyucak, J. Chem. Phys. **132**, 114510 (2010).

[38] B. Hess, C. Holm, and N. van der Vegt, J. Chem. Phys. **124**, 164509 (2006).

[39] J. Li, R. Car, C. Tang, and N. S. Wingreen, PNAS **104**, 2626 (2007).

[40] U. Kaatze, J. Chem. Eng. Data **34**, 371 (1989).

[41] B. Hess, C. Holm, and N. van der Vegt, J. Chem. Phys. **124**, 164509 (2006).

[42] J. Li, R. Car, C. Tang, and N. S. Wingreen, PNAS **104**, 82626 (2007).

[43] C. L. Dias, T. Hynninen, T. Ala-Nissila, A. S. Foster, and M. Karttunen, J. Chem. Phys. **134**, 065106 (2011).

[44] G. Hummer, L. R. Pratt, and A. E. Garca, J. Phys. Chem. **100**, 1206 (1996).